Acta Crystallographica Section D
Biological Crystallography
ISSN 0907-4449

Structural comparison of *Escherichia coli* L-asparaginase in two monoclinic space groups

Mario Sanches,[a] João Alexandre R. G. Barbosa,[b] Ricardo Toledo de Oliveira,[b] José Abrahão Neto[c] and Igor Polikarpov[a,b]*

[a]Grupo de Cristalografia, Departamento de Física em São Carlos, USP, Av. Trabalhador SãoCarlense 400, CEP 13560-970, São Carlos/SP, Brazil, [b]Laboratório Nacional de Luz Síncrotron (LNLS), CP 6192, CEP 13084-971, Campinas/SP, Brazil, and [c]Departamento de Bioquímica e Technologia Farmacêutica, Escola de Ciencias Farmacêuticas, Universidade de São Paulo, SP, Brazil

Correspondence e-mail: ipolikarpov@if.sc.usp.br

Received 29 October 2002
Accepted 19 November 2002

PDB Reference: L-asparaginase, 1nns, r1nnssf.

The functional L-asparaginase from *Escherichia coli* is a homotetramer with a molecular weight of about 142 kDa. The X-ray structure of the enzyme, crystallized in a new form (space group $C2$) and refined to 1.95 Å resolution, is compared with that of the previously determined crystal form (space group $P2_1$). The asymmetric unit of the new crystal form contains an L-asparaginase dimer instead of the tetramer found in the previous crystal form. It is found that crystal contacts practically do not affect the conformation of the protein. It is shown that subunit *C* of the tetrameric form is in a conformation which is systematically different from that of all other subunits in both crystal forms. Major conformational differences are confined to the lid loop (residues 14–27). In addition, the stability of this globular protein is analyzed in terms of the interactions between hydrophobic parts of the subunits.

1. Introduction

L-Asparaginase is an enzyme that catalyses the hydrolysis of L-asparagine to L-aspartate and ammonia. Asparaginases are expressed in many bacterial organisms and the crystallographic structures of asparaginases from *Erwinia chrysanthemi* (Miller *et al.*, 1993), *Pseudomonas* 7a (Lubkowski, Wlodawer, Ammon *et al.*, 1994), *Wolinella succinogenes* (Lubkowski *et al.*, 1996) and *Escherichia coli* (Swain *et al.*, 1993; Polikarpov *et al.*, 1999) have been described. Two L-asparaginases, namely asparaginases I and II, have been isolated from *E. coli*. Type II L-asparaginase is located near the cell surface and is highly active against asparagine-deficient tumours in mammals, whereas type I L-asparaginase is constitutive and does not inhibit tumour growth (Cedar & Schwartz, 1967). Type II L-asparaginase is a chemotherapeutic agent used in the treatment of paediatric acute lymphoblastic leukaemia. Its effectiveness comes from the rapid and complete depletion of circulating asparaginase. However, the treatment is limited by its toxicity, multiple side effects and spontaneous resistance (Chakrabarti & Scuster, 1997).

The active *E. coli* L-asparaginase acts as a homotetramer of 142 kDa, with 326 amino-acid residues per subunit (Epp *et al.*, 1971). Each subunit of the tetramer makes two types of contact with the neighbouring subunits. One could be called an intimate contact, leading to formation of the intimate dimer (Swain *et al.*, 1993), and the other could be termed a distant contact, forming the distant dimer. The intimate dimer accommodates two separate active sites in its interface. All but one of the L-asparaginases structurally determined to date crystallize with a homotetramer or a homodimer of the enzyme in the asymmetric unit cell, with L-asparaginase–glutaminase from *Acinetobacter glutaminasificans* being the

only exception. This enzyme crystallized in the orthorhombic space group $I222$, with a monomer in the asymmetric unit (Lubkowski, Wlodawer, Housset *et al.*, 1994). In this case, the functional tetramer could be generated by crystal symmetry operations. L-asparaginase from *E. coli* was originally crystallized in the monoclinic space group $P2_1$, with a homotetramer in the asymmetric unit. The structure was refined to 2.4 Å resolution (PDB code 3eca; Swain *et al.*, 1993). We will refer to this crystal form as crystal form *A*. Structures of mutants T98V and Y25F in the space groups $P2_12_12_1$ and $P6_522$, respectively, have also been determined (Palm *et al.*, 1996; Jaskólski *et al.*, 2001).

Native L-asparaginase from *E. coli* was crystallized in our laboratory in a different monoclinic space group ($C2$; Polikarpov *et al.*, 1999), which we will subsequently refer to crystal form *B*. Crystal form *B* contains two subunits of the enzyme (a dimer) in the asymmetric unit. The purpose of this paper is to report the structure of the native L-asparaginase in crystal form *B*, refined to 1.95 Å resolution, and to compare it with the crystal form *A* structure.

Table 1
Crystallographic data and statistics for L-asparaginase (crystal form *B*).

Values in parentheses are for the last resolution shell (2.0–1.95 Å).

Crystal dimensions (mm)	0.5 × 0.3 × 0.2
Space group	$C2$
Unit-cell parameters (Å, °)	a = 76.3, b = 134.6, c = 64.8, β = 110.5
Z (No. of chains in a.u.)	2
V_M (Matthews coefficient)	2.19 Å^3 Da^{-1}
Resolution (Å)	13.0–1.95
$I/\sigma(I)$	12.7 (2.4)
Completeness (%)	91.8 (93.2)
R_{merge} (%)	4.7 (32.5)
R factor (%)	13.4
R_{free} (%)	17.4
Unique reflections	40.782
Observed reflections	63.394
Ramachandran plot	
Most favoured (%)	92.8
Allowed (%)	6.5
Generously allowed (%)	0.4
Disallowed (%)	0.4
R.m.s.d. bond lengths (Å)	0.014
R.m.s.d. bond-angle distances (Å)	0.032

2. Materials and methods

2.1. Crystallization and data-collection

Crystallization of *E. coli* L-asparaginase in crystal form *B* has been described in Polikarpov *et al.* (1999). Briefy, L-asparaginase purchased in a lyophilized form from Merck, Sharp and Dohme was crystallized using a sparse-matrix screen at 291 K. The crystals were grown using the hanging-drop vapour-diffusion technique by mixing equal volumes of 20 mg ml^{-1} protein solution and of reservoir solution containing 30% 2-methyl-2,4-pentanediol, 4% PEG 3350, 0.1 *M* 2-(*N*-morpholino)ethanesulfonic acid buffer pH 6. Crystals of dimensions 0.5 × 0.3 × 0.2 mm appeared after one week.

2.2. Data collection and refinement

X-ray diffraction data were collected at the dedicated protein crystallography beamline at the Brazilian National Synchrotron Light Laboratory (Polikarpov, Oliva *et al.*, 1998; Polikarpov, Perles *et al.*, 1998). The data were processed using *DENZO* and *SCALEPACK* (Otwinowski, 1993). The structure was solved by the molecular-replacement method with *AMoRe* (Navaza, 1994), using a distant dimer of crystal form *A* L-asparaginase as the search model. The rotation function was calculated using diffraction data in the resolution range 10.0–4.0 Å and a Patterson radius of 36 Å. The translation search was performed using the Crowther and Blow translation function (Crowther & Blow, 1967). Both rotation and translation searches resulted in clear solutions well above the noise level (Polikarpov *et al.*, 1999). Further positional and *B*-factor refinement was performed with *REFMAC* and *REFMAC*5 (Murshudov *et al.*, 1997). Water molecules were inserted with *ARP*/*wARP* (Lamzin & Wilson, 1993). Details of the data-collection statistics and refinement are given in Table 1. The final calculated electron density was of excellent

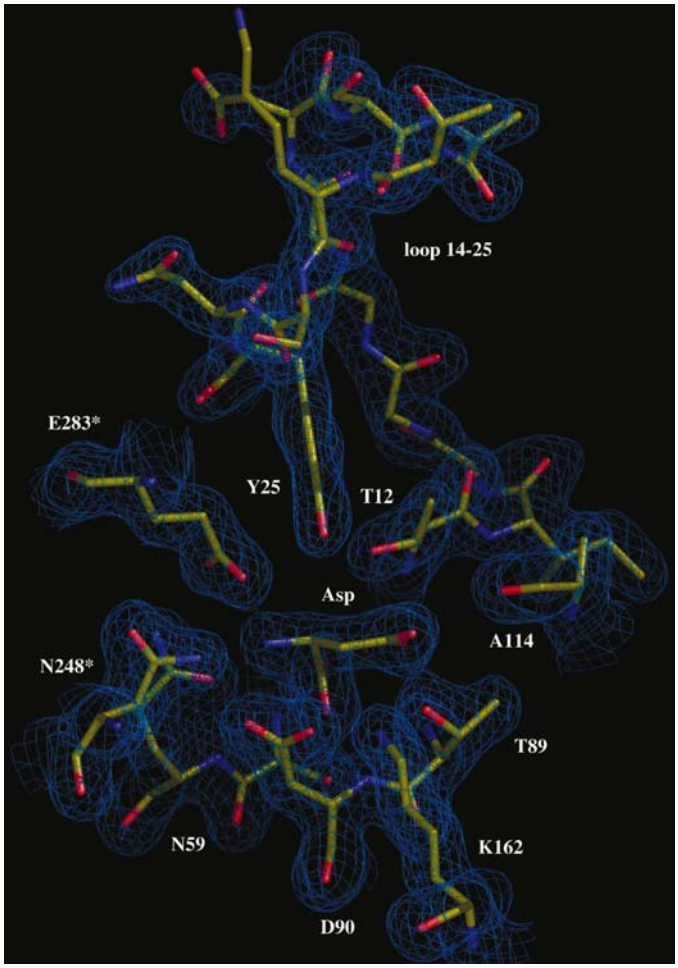

Figure 1
Representative part of the electron density together with the respective part of the crystallographic model. Asterisks mark residues that belong to a neighbouring subunit.

quality for all the present crystallographic model, except perhaps for the flexible loop (residues 14–27) (see Fig. 1).

2.3. Structure comparison and analyses

In crystal form *B*, the functional tetramer of L-asparaginase is located on the twofold crystallographic axis. Therefore, the contents of the asymmetric unit comprise a dimer. For the purpose of comparison with crystal form *A*, a tetramer was generated using the program *O* (Jones & Kjeldgaard, 1993) by applying *C*2 symmetry operations to the crystallographically independent dimer. Subunits *A* and *B* are crystallographically related to subunits *C* and *D*, respectively. The root-mean-square deviations (r.m.s.d.s) were calculated using the program *LSQKAB* (Collaborative Computational Project, Number 4, 1994). Intermolecular and intersubunit contacts were calculated for both crystal forms using the program *CONTACT* (Collaborative Computational Project, Number 4, 1994). Only contacts with some probability of forming hydrogen bonds, according to the program, were considered. The program uses a simple bricking algorithm, where every atom is placed in a 6 × 6 × 6 Å box and the contacts are limited to neighbouring boxes. Hydrogen bonds are assigned to every contacting donor/acceptor pair. Interfacial hydrogen bonds were calculated using the program *DIMPLOT* (Wallace *et al.*, 1995), which employs the program *HBPLUS* with a somewhat more elaborate algorithm. The program first determines the theoretical positions of the H atoms relative to each possible donor, using the ideal hybridization angle to the given atom. Each donor/acceptor pair is then analyzed with respect to its distances and angles. Those that match the limits stipulated by the program are considered to be high-probability hydrogen bonds. Secondary-structure elements were assigned by *PROCHECK* (Laskowski *et al.*, 1993). The buried area (BA) was obtained using the accessible surface area (ASA) calculated using the program *NACCESS* (Hubbard & Thornton, 1993). ASA was calculated for each subunit, each dimer (distant and intimate) and the whole molecule. The buried area was calculated using the expression $BA_{xy} = (ASA_x + ASA_y) - ASA_{xy}$, where ASA_x and ASA_y were calculated for each separate interacting chain and ASA_{xy} was calculated for both. The theoretical number of hydrogen bonds per Å^2 is given by $n = 5.34s \times 10^{-3}$ Å^2, where s is the buried area of the interface (Xu *et al.*, 1997).

Planarity was calculated using the program *SURFNET* (Laskowski, 1995). The r.m.s.d.s of all the interface atoms from the least-squares plane through all these atoms was calculated. The gap index (GI) was calculated using the expression GI = GV − ASA, where GV is the gap volume between the interfaces, which was also calculated using the program *SURFNET* (Laskowski, 1995).

3. Results and discussion

3.1. Structure description

The structure of an L-asparaginase subunit consists of two α/β domains (Swain *et al.*, 1993). The N-terminal flavodoxin-like domain contains nine α-helixes and ten β-strands and the C-terminal domain consists of five α-helices and four β-strands. In each domain there is a parallel β-strand core which forms a twisted plane involving α-helices. The connection between the N- and C-terminal domains is achieved by a random-coil sequence encompassing residues 201–213. There is a single disulfide bond in each subunit, connecting Cys77, which is located in a random coil between Nα5 and Nα6, and Cys105, which is located in a random coil between Nα7 and Nα4. A structural cartoon of the subunit is given in Fig. 2.

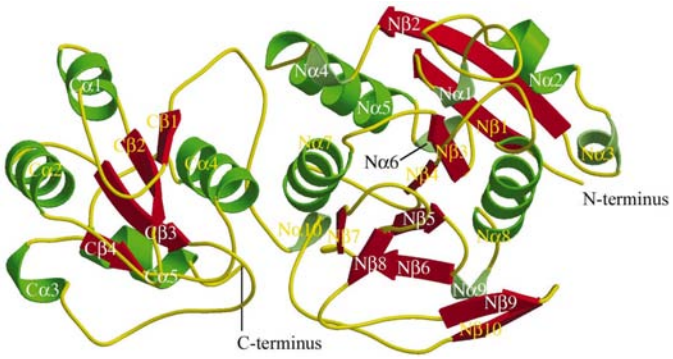

Figure 2
A schematic representation of the *E. coli* L-asparaginase subunit produced using *MOLSCRIPT* (Kraulis, 1991). Secondary structures marked N belong to the N-terminal domain and those marked C belong to the C-terminal domain. The 3_{10}-helices Nα1, Nα3, Nα6 and Nα10 are shown in opaque green.

Figure 3
A graphical representation of the L-asparaginase tetramer produced using *MOLSCRIPT* (Kraulis, 1991). Intimate dimers are formed by subunits drawn in yellow/blue and green/pink.

Table 2
Main-chain, side-chain and all-atom r.m.s.d.s (in Å), respectively, between all subunits of the two structures.

The crystal form is indicated in parentheses.

Chains	*B* (form *B*)	*A* (form *A*)	*B* (form *A*)	*C* (form *A*)	*D* (form *A*)
A (form *B*)	0.095, 0.797, 0.548	0.317, 0.910, 0.663	0.360, 1.138, 0.821	0.493, 1.163, 0.871	0.366, 1.228, 0.880
B (form *B*)		0.322, 1.121, 0.800	0.361, 0.903, 0.671	0.499, 1.194, 0.892	0.374, 1.237, 0.887
A (form *A*)			0.287, 1.118, 0.791	0.432, 1.178, 0.864	0.284, 1.225, 0.861
B (form *A*)				0.373, 1.180, 0.851	0.304, 1.222, 0.863
C (form *A*)					0.426, 1.252, 0.910

Table 3
R.m.s.d.s (in Å) for the loop between residues 14 and 27, comparing the same subunit of the two crystal forms.

Chain loop	Main chain	Side chain	All atoms
A	0.368	1.447	0.992
B	0.701	1.991	1.400
C	0.985	2.109	1.562
D	0.616	1.854	1.293

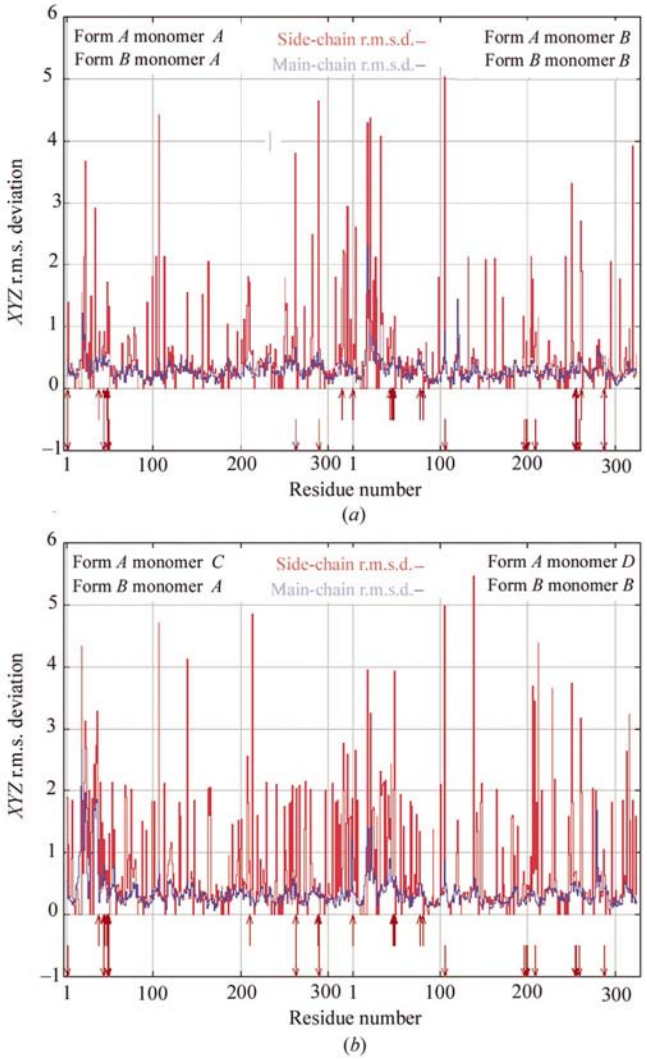

Figure 4
R.m.s.d.s between each related subunit of both crystal forms. Below each plot there is a schematic representation of the crystalline contacts. Each amino acid engaged in a crystalline contact is represented by an arrow: up arrows indicate form *A* and down arrows indicate form *B*.

Each L-asparaginase tetramer contains four active sites. The active sites are located at the interface between two subunits forming an intimate dimer (Swain *et al.*, 1993); there are two active sites per interface. The distant dimer interface does not contain active sites. The molecule assembles in a tetramer which may therefore be described as a dimer of dimers (Fig. 3). Crystal form *B* contains one distant dimer (*A*–*B*) in the asymmetric unit. Another distant dimer (*C*–*D*) in crystal form *B* resides in a neighbouring asymmetric unit. The intimate dimers *A*–*C* and *B*–*D* are related by a twofold crystallographic axis in this particular crystal form. The only two residues in disallowed regions of the Ramachandran plot are Thr198 of both subunits, both of which display a perfect fit to the electron density. The reason for the deviation from the allowed conformation seems to be the hydrogen-bonded interaction of Thr198 OG1 with a water molecule coordinated by His197 O and Ser199 OG. The form *B* structure has a slightly higher number of water molecules compared with form *A* (658 per tetramer in form *B* compared with 410 in the form *A* tetramer). This difference may be attributed to the higher resolution of form *B*. The r.m.s.d.s between the subunits in the two structures are given in Table 2. As can be seen, one chain (subunit *C*) systematically presents r.m.s.d. values that are somewhat higher than those of the other chains. The r.m.s.d.s for the subunit *C* main-chain atom positions compared with all other subunits of both crystal forms are 0.452 ± 0.051 Å, whereas the r.m.s.d.s of the main-chain atoms of all other subunits superimposed pairwise amongst themselves are 0.336 ± 0.097 Å. The r.m.s.d.s for the whole tetramer are 0.46 Å (main chain), 1.09 Å (side chains) and 0.81 Å (all atoms) between crystal forms *A* and *B*. The highest r.m.s.d.s correspond to the loop between residues 14 and 27 (Table 3). Electron density in this region is poor in both crystal forms (Swain *et al.*, 1993). Here, chain *C* clearly stands out as having the highest r.m.s.d. values. Graphical representations of the r.m.s.d.s between each related subunit of both crystal forms are given in Fig. 4. Disorder in the region of the loop (residues 14–27) can also be seen from the *B*-factor plot (Fig. 5). The *B* factors of the polypeptide chains are particularly high in this region and are quite different for all four chains in crystal form *A*, with chain *A* having the lowest *B* factors and chain *C* presenting the highest *B* factors. Remarkably, the thermal parameters of the ligand L-asparagine vary from subunit to subunit in a similar way, being most disordered in subunit *C*. *B*-factor plots for each of the crystallographically independent subunits in the crystal form *B* are very similar, although no *B*-factor NCS restraints were applied during the refinement.

3.2. Conformation and stability

Even though the intimate dimer theoretically possesses all the necessary conditions for activity, L-asparaginases act as

Table 4
Surface–surface interaction parameter calculations.

The parameters were calculated for each possible interaction between two subunits of the tetramer of crystalline form *B*.

Interaction	BA† (Å^2)	%‡	n_T§	n_D§	*P*¶ (Å)	GI†† (Å)	Type
AC	4667.73	16.28	25	28	6.22	1.72	Intimate
BD	4689.65	16.09	25	30	6.12	1.82	Intimate
AB = *CD*	1877.95	6.55	10	7	2.70	2.76	Distant
AD	2049.83	7.12	11	16	2.84	2.86	Distant
BC	2049.76	7.06	11	16	2.84	2.83	Distant

† Buried area. ‡ The percentage refers to the amount of area buried between the two interactive parts compared with the sum of the total accessible surface area of each subunit alone. § The theoretical number of hydrogen bonds by interface (n_T, hydrogen bonds per Å^2) and this number determined using the program *HBPLUS* (McDonald & Thornton, 1994) (n_D, hydrogen bonds per Å^2). ¶ Planarity. †† Gap index.

tetramers. Why then does the enzyme assemble in tetramers under physiological conditions? The tetrameric assembly of the protein under physiological conditions may be explained, at least partially, by the nature of the dimeric interface interactions. The interface between intimate dimers (*i.e.* the interface between dimer *AC* and a dimer *BD*) can be seen in Figs. 6(*a*) and 6(*b*). It is clear that the interaction surface is mainly hydrophobic, with the majority of the charged and polar residues being in contact with solvent on the external surface of the enzyme. In line with the results of Jones & Thornton (1996), the interaction between the dimers bears the characteristics of physiologically relevant complexes, being more hydrophobic and presenting low intersubunit hydrogen-bond content, as can be seen in Table 4. The tetramer keeps the most hydrophobic part of the protein buried inside of its core, away from contact with solvent, providing stabilization and rendering a globular-shaped molecule, with the polarizable surface oriented towards the external medium (Figs. 6*b* and 6*c*).

L-Asparaginases are very stable enzymes which preserve their activity over a wide pH (4.5–11.5) and temperature range (Stecher *et al.*, 1999; Cammack *et al.*, 1972). Moreover, on being exposed to extreme pH and brought back to physiological pH, the enzyme activity is restored (Stecher *et al.*, 1999; Cammack *et al.*, 1972). The very robust active sites are buried in the interface between the intimate dimers (see *BA* in Table 4) and are not directly affected by pH changes. Above and below the range of pH stability, the side chains of charged residues are considerably affected (deprotonated or protonated) and therefore presumably interfere with the intramolecular electrostatic interactions, protein folding and subunit assembly.

The buried area between subunits forming intimate dimers is composed of about 56% non-polar residues and represents about 16% of the total area of the subunits of an intimate dimer (Table 4). Comparison of the two crystal forms, *A* and *B*, shows that there is no significant difference in buried area between them, indicating that they are not affected by crystal packing. The theoretical accessible surface area is given by the expression ASA = $6.3m^{0.73}$ Å^2, where *m* is the molecular mass of the subunit or oligomer (Miller *et al.*, 1987). The area buried upon formation of the oligomer can be calculated using this expression as the difference between the total surface of the exposed areas of subunits composing the oligomer and that of the oligomer itself. Theoretically, the area buried upon formation of a dimer calculated in this manner from two subunits with a molecular mass of 35.5 kDa is equal to 4510 Å^2, which is very close to the buried area for the intimate dimers calculated on the basis of the crystallographic model (4660 Å^2).

The interacting surface area in an intimate dimer shows a relatively high deviation from planarity and a low gap index (Table 4), indicating a strong interaction between the molecules. The number of hydrogen bonds between subunits forming the intimate dimers calculated using *HBPLUS* is slightly higher than the expected theoretical value (Table 4). The same is observed for distant interaction between subunits *AD* and *BC*, respectively. The other two interactions, *AB* and *CD*, present fewer hydrogen bonds than expected, owing to the apolar nature of this interaction. This pattern suggests that

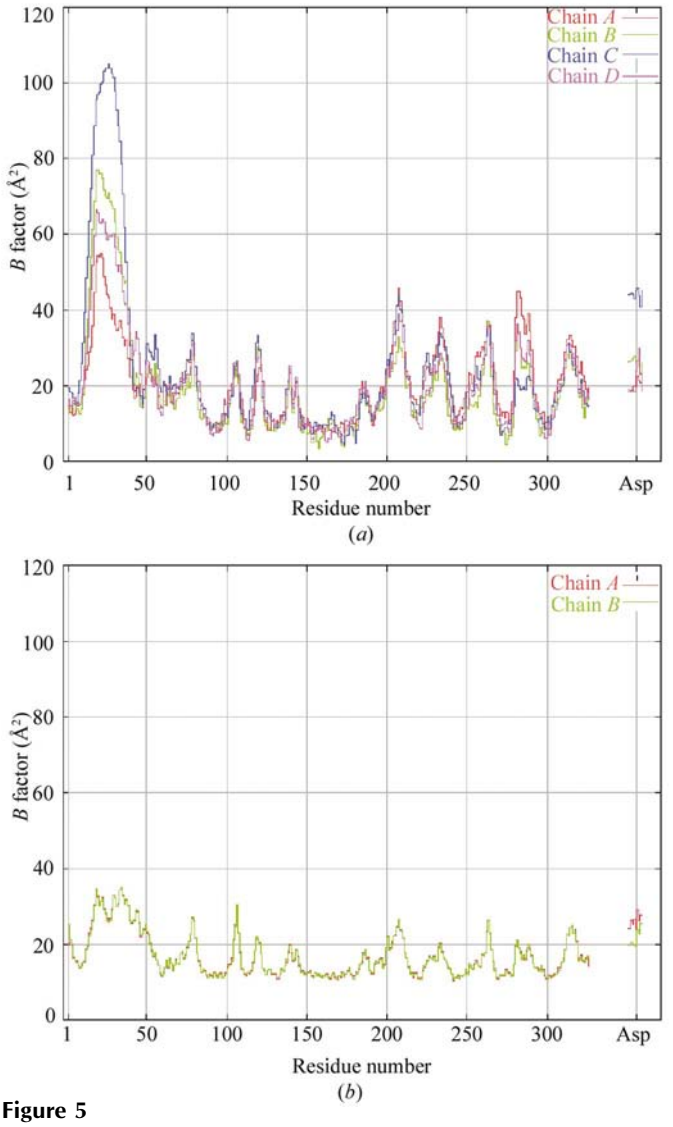

Figure 5
B factors of C$^\alpha$ positions. (*a*) Form *A*, (*b*) form *B*. The separated plot, marked Asp, at the very right of the figure represents *B* factors of all atoms of the ligand aspartate.

the tetrameric assembly can be viewed as an association of two intimate dimers maintained mainly by *AD* and *BC* interactions. Additionally, according to the study of Xu *et al.* (1997), there are an average of two salt bridges per interface. The intimate dimer assembly matches this value, with the strong interactions on interfaces *AD* and *BC* including six possible salt bridges compared with none on the other two interfaces.

3.3. Crystal contacts

Crystal contacts are quite different in crystal forms *A* and *B*. The amino-acid residues involved in these contacts are flagged at the bottom of Fig. 4. Monomer *C* of crystal form *A* participates in 14 crystal contacts, compared with the eight, 11 and nine contacts in which subunits *A*, *B* and *D* are involved, respectively. Of these 14 contacts, seven are specific to this subunit (not observed in other subunits) compared with one, four and three specific contacts of subunits *A*, *B* and *D*, respectively. The crystal form *B* subunits (chains *A* and *B*) are involved in nine crystalline contacts each. All of these contacts are specific. In contrast, the non-crystallographic contacts are very similar in all subunits of both crystal forms.

The r.m.s.d.s calculated only for residues involved in crystallographic contacts amount to 0.46 Å for the main-chain atoms, 1.79 Å for the side-chain atoms and 1.30 Å for all atoms. Interestingly, the r.m.s.d. for the main-chain atoms of residues involved in the crystallographic contacts is exactly the same as for all main-chain atoms of the protein. Also, significant differences in r.m.s.d. are only observed for the side-chain atoms (Table 2 and §3.1). This indicates that the conformational differences of the side chains induced by the crystalline lattice do not affect the conformation of the protein to any great extent.

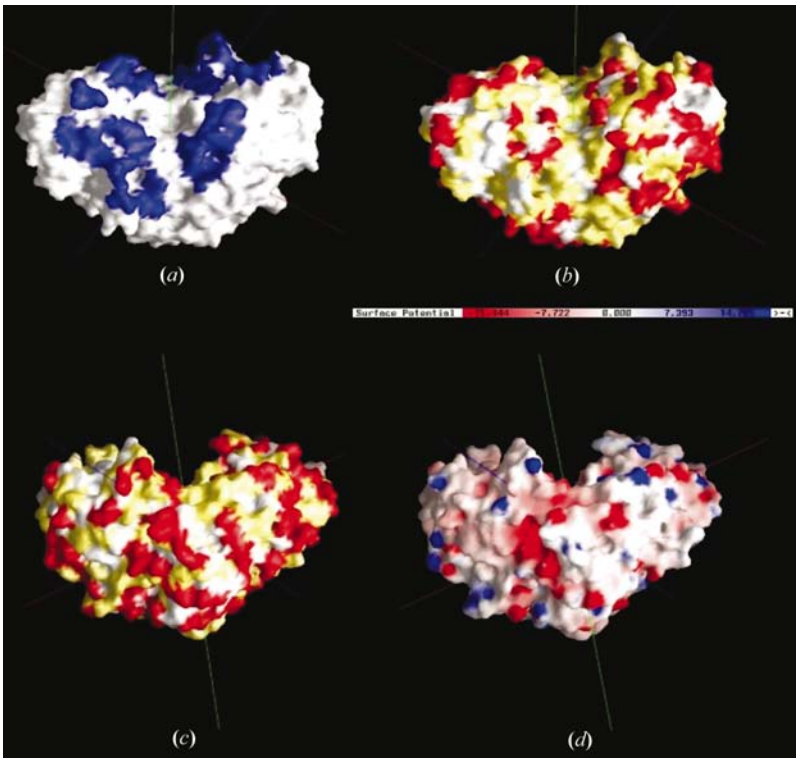

Figure 6
GRASP (Nicholls *et al.*, 1991) representation of the molecular surface of the intimate dimer (*A*–*C*). (*a*) The blue area shows the contact surface between two intimate dimers in the range 2.5 Å. (*b*) The same view as in (*a*), but showing hydrophobic residues in white, polar residues in yellow and charged residues in red. (*c*) External part of the dimer. Hydrophobic areas are white, polar areas are yellow and charged niches are red. (*d*) The same point of view as in (*c*), but showing an electrostatic potential surface.

4. Conclusions

The detailed crystallographic comparison of the two crystal forms of native *E. coli* L-asparaginase presented in this paper demonstrates that the enzyme conformation is not significantly affected by crystallographic contacts. No significant conformational changes in protein structure are observed. The only exception seems to be subunit *C* of the tetramer in crystalline form *A* (space group $P2_1$). The 14–27 loop of this subunit systematically presents higher r.m.s.d.s compared with the subunits in the other crystal form as well as the other subunits of the same tetramer (Table 3). Moreover, the 14–27 loop is more flexible or disordered in this particular subunit compared with the same loop of the rest of the tetramer and the dimer of crystal form *B*. This loop is proposed to be involved in the reaction process (Swain *et al.*, 1993; Palm *et al.*, 1996), probably acting as a lid to the active site. Moreover, the crystal contacts of the subunit *C* are very specific, indicating a systematic difference of this subunit compared with the other three subunits of the same tetramer. There could be two explanations for this phenomenon. First of all, the subunit *C* conformation may be affected by the crystalline contacts. The second explanation is that subunit *C*, even in solution before crystallization, was (and continues to be) in a particular conformation different from that of all the other subunits. This conferred the specific orientation of the L-asparaginase tetramer selected during the molecular crystal assembly and growth and therefore the particular position of subunit *C*. We strongly favour the second hypothesis. There are several arguments in support of this hypothesis. First of all, the r.m.s.d.s of the subunit *C* polypeptide chain are not correlated with the crystalline contact positions (Fig. 4 and Tables 2, 3 and 5). Secondly, the temperature factors of the lid loop 14–27 and the ligand for this particular subunit are significantly higher then the *B* factors of the same loop and the ligands of the rest of subunits in both crystal forms (Fig. 5). Since the occupancy of the ligand was set to 1, the *B* factors represent both its disorder and its low occupancy. Thirdly, the *E. coli* enzyme contains an average of three molecules of L-aspartic acid per molecule of tetramer (*i.e.* per four molecules of subunits; Jayaram *et al.*, 1986) and it is tempting to propose that the occupancy of

the ligand in the active site of one particular subunit (subunit *C*) is very low. Lastly, this explains the high factors of the lid loop (residues 14–27), which is more disordered in the apo enzyme (Lubkowski *et al.*, 1996). This loop serves as a flexible lid that mediates the access of the ligand to the active site, as observed previously in the L-asparaginase from *W. succinogenes* (Lubkowski *et al.*, 1996).

The stability of the tetramer can be explained in terms of the interface interactions of the subunits. The assembly of the intimate dimers is mainly hydrophobic in nature (Table 4), with a number of characteristics of permanent physiologically relevant complexes (Jones & Thornton, 1996). This indicates that the entropic contribution is important for the assembly of intimate dimers, whereas significant enthalpic contribution seems to arise from the ion-pair interactions on the distant dimer interfaces *A*–*D* and *B*–*C*.

We gratefully acknowledge financial support from Conselho Nacional de Desenvolvimento Cientifico e Tecnológico (CNPq) and from Fundação de Amparo à Pesquisa do Estado de São Paulo (FAPESP), Brazil *via* grants Nos. 99/03387-4, 98/12043-4 and 0/03674-2.

References

Cammack, K. A., Marlborough, D. I. & Miller, D. S. (1972). *Biochem. J.* **126**, 361–379.
Cedar, H. & Schwartz, J. H. (1967). *J. Biol. Chem.* **242**, 3753–3755.
Chakrabarti, R. & Scuster, S. M. (1997). *Int. J. Pediatr. Hematol./Oncol.* **4**, 597–611.
Collaborative Computational Project, Number 4 (1994). *Acta Cryst.* D**50**, 760–763.
Crowther, R. A. & Blow, D. M. (1967). *Acta Cryst.* **23**, 544–548.
Epp, O., Steigemann, W., Formanek, H. & Huber, R. (1971). *Eur. J. Biochem.* **20**, 432–437.
Hubbard, J. S. & Thornton, J. M. (1993). *NACCESS.* Department of Biochemistry and Molecular Biology, University College London.
Jaskólski, M., Kozak, M., Lubkowski, J., Palm, G. & Wlodawer, A. (2001). *Acta Cryst.* D**57**, 369–377.
Jayaram, H. N., Cooney, D. A. & Huang, C. Y. (1986). *J. Enzyme Inhib.* **1**, 151–161.
Jones, S. & Thornton, J. M. (1996). *Proc. Natl Acad. Sci. USA*, **93**, 13–20.
Jones, T. A. & Kjeldgaard, M. (1993). *O Version 5.9, The Manual.* Uppsala University, Uppsala, Sweden.
Kraulis, P. J. (1991). *J. Appl. Cryst.* **24**, 946–950.
Lamzin, V. S. & Wilson, K. S. (1993). *Acta Cryst.* D**49**, 129–147.
Laskowski, R. A. (1995). *J. Mol. Graph. Model.* **13**, 323–330.
Laskowski, R. A., MacArthur, M. W., Moss, D. S. & Thornton, J. M. (1993). *J. Appl. Cryst.* **26**, 283–291.
Lubkowski, J., Palm, G. J., Gilliland, G. L., Derst, C. & Rohm, K.-H. (1996). *Eur. J. Biochem.* **241**, 201–207.
Lubkowski, J., Wlodawer, A., Ammon, H. L., Copeland, T. D. & Swain, A. L. (1994). *Biochemistry*, **33**, 10257–10265.
Lubkowski, J., Wlodawer, A., Housset, D., Weber, I. T., Ammon, H. L., Murphy, K. C. & Swain, M. L. (1994). *Acta Cryst.* D**50**, 826–832.
McDonald, I. K. & Thornton, J. M. (1994). *J. Mol. Biol.* **238**, 777–793.
Miller, S., Lesk, A. M., Janin, J. & Chothia, C. (1987). *Nature (London)*, **328**, 834–836.
Miller, M., Rao, J. K. M., Wlodawer, A. & Gribskov, M. R. (1993). *FEBS Lett.* **328**, 275–279.
Murshudov, G. N., Vagin, A. A. & Dodson, E. J. (1997). *Acta Cryst.* D**53**, 240–255.
Navaza, J. (1994). *Acta Cryst.* A**50**, 157–163.
Nicholls, A., Sharp, K. & Honig, B. (1991). *Proteins Struct. Funct. Genet.* **11**, 281–296.
Otwinowski, Z. (1993). *Proceedings of the CCP4 Study Weekend. Data Collection and Processing*, edited by L. Sawyer, N. Isaacs & S. Bailey, pp. 56–62. Warrington: Daresbury Laboratory.
Palm, G. J., Derst, C., Lubkowski, J., Schleper, S., Rohm, K. H. & Wlodawer, A. (1996). *FEBS Lett.* **390**, 211–216.
Polikarpov, I., Oliva, G., Castellano, E. E., Garratt, R. C., Arruda, P., Leite, A. & Craievich, A. (1998). *Nucl. Instrum. Methods Phys. Res. A*, **405**, 159–164.
Polikarpov, I., Oliveira, R. T. & Abrahão-Neto, J. (1999). *Acta Cryst.* D**55**, 1616–1617.
Polikarpov, I., Perles, L. A., de Oliveira, R. T., Oliva, G., Castellano, E. E., Garratt, R. C. & Craievich, A. (1998). *J. Synchrotron. Rad.* **5**, 72–76.
Stecher, A. L., Deus, P. M., Polikarpov, I. & Abrahão-Neto, J. (1999). *Pharm. Acta Helv.* **290**, 1–9.
Swain, A. L., Jaskolski, M., Housset, D. & Rao, J. K. M. (1993). *Proc. Natl Acad. Sci. USA*, **90**, 1474–1478.
Wallace, A. C., Laskowski, R. A. & Thornton, J. M. (1995). *Protein Eng.* **8**, 177–134.
Xu, D., Tsai, C.-J. & Nussinov, R. (1997). *Protein Eng.* **10**, 999–1012.